



# Monitoring-based adaptive water level thresholds for bridge scour risk management

Andrea Maroni<sup>a</sup>, Enrico Tubaldi<sup>a,\*</sup>, Hazel McDonald<sup>b</sup>, Daniele Zonta<sup>c</sup>

<sup>a</sup> University of Strathclyde, Department of Civil and Environmental Engineering, Glasgow, UK

<sup>b</sup> Transport Scotland, Roads Directorate, Glasgow, UK

<sup>c</sup> University of Trento, Department of Civil, Environmental and Mechanical Engineering, Trento, Italy

## ARTICLE INFO

### Keywords:

Bridge scour risk  
Structural health monitoring  
Bayesian network  
Decision support system

## ABSTRACT

Riverbed scour is the leading cause of bridge failure worldwide. Recent developments in sensor technology for structures have resulted in more bridges being instrumented and monitored. However, alongside scour monitoring systems, there is a need of techniques to handle the data obtained and exploit them to inform the management of the bridge scour risk. This paper illustrates the development of a decision support system (DSS) for bridge scour risk management, which is based on a probabilistic framework for scour risk estimation, enhanced by real-time information from scour monitoring systems and in line with current risk procedures used by transport agencies. The proposed DSS provides bridge operators with adaptive measurement-informed water level thresholds triggering bridge closure to traffic under heavy floods. The application of the DSS is illustrated by considering a case study of three bridges at risk of scour managed by Transport Scotland. It is shown that information from scour sensors within the proposed DSS allows reducing the uncertainty in the scour estimates and yields adaptive water level thresholds triggering bridge closure to traffic that can differ significantly from those currently considered by transport agencies. This can ultimately result in a reduction of false alarms and unnecessary bridge closures.

## 1. Scour risk management

Bridge scour is the removal of material from the bed of streams around bridge foundations under the erosive action of flowing water [1–4]. This phenomenon is responsible for a large number of failures worldwide. For example, in the UK, scour has caused the collapse of almost one bridge per year in the period 1846–2013 [5]. In the US, an average annual rate of 22 bridges was found to collapse or undergo severe damage according to a study by Briaud et al. [6]. Wardhana and Hadipriono [7] also showed that the combined figure of 266 flood/scour-related cases in the US constitutes the most dominant bridge failure cause (53% of the total cases of failures). Climate change is expected to exacerbate the bridge scour risk [8]. For example, according to the UK Climate Change Risk Assessment, considering a medium emission scenario, an increase of 15–20% of failure rates is expected by 2050s [9,10].

Transport agencies responsible for bridge management carry out regular assessments of the scour risk of bridges and assign them risk scores, which are used for planning inspections and prioritising

mitigation interventions. In Scotland, around 8% of the 2029 bridges and culverts over water managed by Transport Scotland (TS) are classified as scour critical and need scour monitoring and protection measures. In the UK, the Procedure BD97/12 [11] is used for evaluating the scour risk of road bridges. The risk evaluation is based on an essentially deterministic approach, which considers a predefined flood scenario (i. e., the 1 in 200-year flood adjusted by an additional 20% on the design flood to account for potential effects of climate change) and employs rather simple models for scour assessment. Moreover, this approach disregards the various uncertainties inherent to the hydraulic and bridge properties, and to the models used for scour assessment [12–14].

Transport agencies also issue action plans, establishing a systematic and structured approach to how they must respond to the threat of adverse weather. The purpose of these documents is to define the decision process and the actions that must be taken during or following an extreme weather event. According to TS's scour management strategy and flood emergency plan, the decision of whether to close a bridge to traffic or not under a heavy flood is made based on the comparison between the water level at the upstream section of the bridge and a

\* Corresponding author.

E-mail address: [enrico.tubaldi@strath.ac.uk](mailto:enrico.tubaldi@strath.ac.uk) (E. Tubaldi).

<https://doi.org/10.1016/j.ress.2023.109473>

Received 31 May 2022; Received in revised form 23 June 2023; Accepted 24 June 2023

Available online 25 June 2023

0951-8320/© 2023 The Authors. Published by Elsevier Ltd. This is an open access article under the CC BY license (<http://creativecommons.org/licenses/by/4.0/>).

critical water level, represented by a marker installed on the bridge. This critical threshold corresponds to the water level expected in correspondence of a specific return period of the flood that is likely to cause damage (i.e., 200 years return period), but can also be defined considering other potential problems for the bridge (e.g., deck uplifting or inundation). Nevertheless, the critical water level cannot directly be associated to a precise level of scour at the bridge foundations because there is not a unique correspondence between scour depth and water levels. In fact, different hydraulic processes can generate the same scour depth at a bridge pier. Moreover, scour can accumulate under multiple flood events [13,14]. Finally, the models employed for evaluating scour are inaccurate and affected by many uncertainties that must be taken into account in the scour assessment. As a result of this, the probability of collapse of a bridge due to scour may differ significantly from the probability of exceedance of the critical water level [2].

For the reasons discussed above, current emergency and long-term scour risk management approaches should be improved, (i) by adding a more explicit consideration of the various sources of uncertainty that affect the problem, thus enabling the shift from a deterministic to a probabilistic evaluation of the scour risk, and (ii) by integrating in the risk assessment the observations from monitoring sensors, allowing the reduction of the uncertainty in the scour risk estimates, and thus helping bridge operators in taking the optimal decisions concerning bridge scour risk management [15].

Bridge scour monitoring is widely recognised as an important scour mitigation measure, e.g., Argyroudis et al. [16] and Tubaldi et al. [4], Giordano et al. [15]. Many sensors have been developed and tested to achieve more precise evaluations of the extent of scour at bridge foundations and of the relevant effects on the performance of bridge components. Reference can be made to Prendergast and Gavin [17], Maroni et al. [18], Achillopoulou et al. [19] and Tubaldi et al. [20] for a review of these. Alongside the development of monitoring systems for bridge scour monitoring, there is also a need of techniques to handle the data obtained from sensors and provide bridge owners and managers with useful information for optimal management of bridge scour. Bayesian Networks (BNs) have already been employed in the context of flood risk assessment of bridges. For example, Martínez-Martínez et al. [21] developed a BN-based framework for the risk assessment of masonry bridge pier failure due to a combination of drag forces and scour in presence of woody debris trapping phenomena. The proposed framework provides a quantitative support to bridge maintenance and inspection strategies. Maroni et al. [22] developed a BN-based approach for propagating the information from available scour probes and gauging stations to update the probabilistic distribution of scour at the foundations of different bridges in a network. However, this framework must be further developed to exploit the reduction of uncertainty stemming from available observations to support the decision-making process.

In this paper, a Decision Support System (DSS) is developed for bridge scour management, which extends and complements current scour risk rating procedures and action plans of transport agencies by enabling the use of monitoring data in the decision-making process. The DSS produces measurement-informed thresholds of the river flow depth triggering bridge closure to traffic under heavy floods, based on the updated estimates of the probabilistic distribution of scour obtained by introducing sensor observations in the BN developed by Maroni et al. [22].

The rest of the paper is structured as follows: Section 2 presents the procedures currently followed by TS to classify bridges at risk of scour and their emergency plans providing the actions to be implemented in the case of an extreme weather event. Section 3 presents the proposed monitoring-informed DSS for bridge scour risk management. Section 4 describes the application of the DSS to a case study consisting of three bridges managed by TS in South-West Scotland and discusses the obtained results by highlighting the changes to current risk management procedures. The paper ends with a conclusion and future works section.

## 2. Current procedures for scour risk assessment and management

In the UK, the assessment of the scour risk at highway and railway structures is carried out in accordance with the Procedure BD 97/12 (Highway [11]). This procedure introduces a bridge scour risk classification based on the relative scour depth  $D_R$ , which denotes the ratio between the total scour depth  $D_T$  and the foundation depth  $D_F$  (Fig. 1). The total scour depth  $D_T$  is defined as the sum of constriction and local scour depth, respectively  $D_C$  and  $D_L$ . The BD97/12 provides the formula for estimating these by starting from an assessment flow, i.e., the flow corresponding to a return period of 200 years. Furthermore, a priority factor  $PF$  is used in the scour risk rating to account for several factors, such as the history of scour problems, the type of foundation, and the importance of the bridge (i.e., vehicle traffic volume). For instance, for  $PF = 2$ , the scour risk classes are defined by the value of  $D_R$  as follows: Class 5 for  $D_R \leq 1$ , Class 4 for  $1 < D_R \leq 1.8$ , Class 3 for  $1.8 < D_R \leq 2.3$ , Class 2 for  $2.3 < D_R \leq 3.5$ , and Class 1 for  $D_R > 3.5$ . It is noteworthy that the use of the models of BD97/12 is likely to result in an overestimation of the scour depth. This explains values of  $D_R$  significantly higher than 1 that can be observed in the scour risk classification of Fig. 1. Nevertheless, values of  $D_R > 1$  may not necessarily result in foundation and bridge collapse due to the shape of the scour hole. This issue is discussed in detail in Tubaldi et al. [4].

In Scotland, TS has also issued a plan describing the actions to be taken during or after the occurrence of a flood event and furnishing a systematic and structured approach to how to respond to the threat of adverse weather [23]. A “visual” decision scheme is employed, which is based on the comparison between the water level and the markers placed on the bridge’s upstream surface.

Two different marker plates are used, the Flood Level Marker (FLM) plate that corresponds to the 1 in 200-year flood level according to the BD97/12 (Fig. 2(a)), and the Red Plate. This latter is installed at the level of the bridge soffit in those structures where the 1 in 200-year flood level is higher than this (Fig. 2(b)). This marker provides a warning for deck uplift, inundation, or no freeboard, risking debris impact.

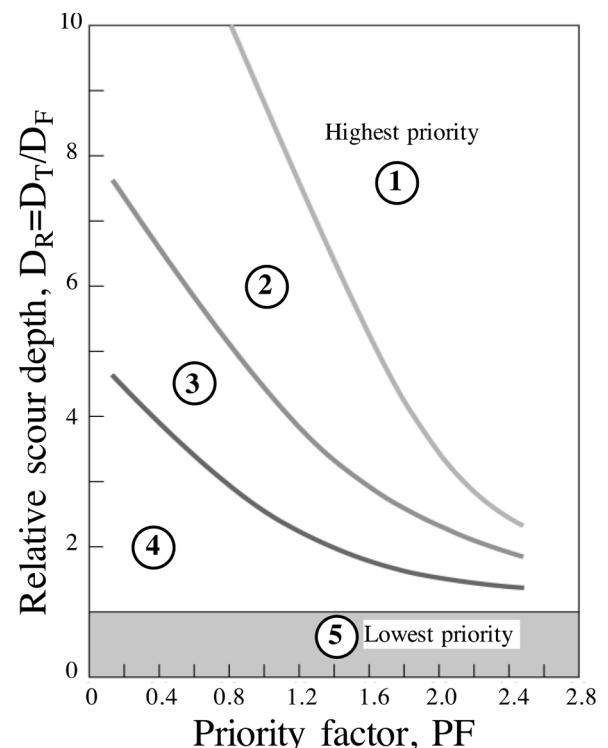


Fig. 1. Scour risk classification performed according to BD97/12.

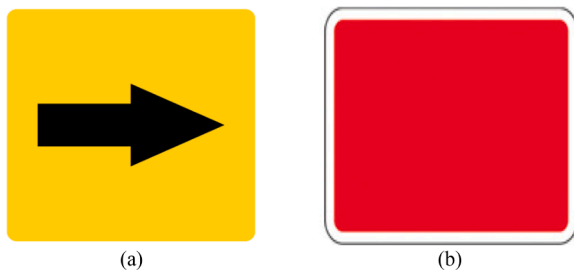


Fig. 2. (a) The Flood Level Marker plate and (b) the Red Plate.

**Table 1**  
Water level safety actions for structures managed by TS.

Markers	Water level	Action
Yes	Below the FLM	Carry out observations
	At the FLM or above it	Close structure
No	Below the Red Plate	Carry out observations
	At the Red Plate or above it	Close structure

When the water exceeds the levels shown on these markers, specific actions such as closure of the bridge to traffic, must be taken (see Table 1). Following the closure, inspection of the structure, including underwater parts and the riverbed, is undertaken as soon as it is safely practicable to do so, and the bridge may be re-opened to traffic once water levels have reduced sufficiently and only if there are no visible signs of deformation or structural distress. The bridge may have to be closed for many days, thus resulting in significant downtime.

In summary, the action plan specifies that any high-risk structure must be closed when the water level reaches a critical threshold at which the bridge is deemed to be at risk of failure. The threshold's choice is conservative by nature, so that safety of road users can be ensured by closing the bridge before the water level rises to a point at which serious scour is likely to develop. However, this plan does not consider the complexity in the temporal evolution of the scour process. For instance, in the case of live-bed regime, soil material may be partially redeposited in the scour depth at the end of the flood [24]. Thus, measurements of scour carried out at the end of a flood may not capture the maximum scour that occurred during the event as the scour hole might have partly filled during the recession [25].

Furthermore, scour depth formula are often very conservative [12, 26,27], being based on laboratory experiments and the assumption that the designed flood acts over an infinite duration [2], while real flood events are characterised by different hydrograph duration and magnitude. Thus, high-flow events may not necessarily result in the development of a significant scour hole, especially if they have a short duration. Moreover, bridges are exposed to sequences of flood events, each potentially contributing to scouring. Thus, their safety could be jeopardized by the progressive accumulation of scour under multiple events with low return period (i.e., water levels below the FLM) occurring in sequence, as was the case of the Lamington viaduct [28].

For the reasons above, the 1 in 200-year flood level marker alone is only a very rough indicator of the scour risk, which remains unknown until the flood has receded, thus allowing divers, sonar or probing surveys to safety check the bridge foundations. More accurate, real-time scour evaluations are required to improve the flood emergency management for bridges and avoid risk misclassifications, unnecessary bridge closures, and excessive downtime.

### 3. Formulation

This section illustrates a decision support system that aims to improve current bridge flood emergency management systems by exploiting monitoring data for making better-informed decisions

concerning bridge closure under heavy floods. In particular, we define an adaptive water level threshold based on information from monitored scour depths and water levels upstream of the bridge.

#### 3.1. Predictive model

In order to apply this framework, we need to state a model that allows prediction of the scour depth  $D_R$  based on water level  $y_U$ . An extensive number of studies has been carried out during the last decades on the physics and modelling of the scour phenomenon. Several approaches have been followed in order to focus on topics such as physical modelling, controlling dimensionless scour parameters or scour estimates including empirical models, numerical frameworks and non-deterministic approaches [2]. However, the main goal of every study is to find a model to predict such a complex phenomenon as the problem of scour at bridge foundations and then manage the risk of scour bridge failure.

In this work, we use the same probabilistic predictive model developed by Maroni et al. [22] for bridge scour hazard assessment and updating, and the same classification scheme of current procedures of transport agencies, which were described in the previous section. Therefore, using epistemological terms, three different inference cases are analysed in the predictive model:

- 1) a *prior* inference of the scour depth based on the sole observation of the water level  $y_U$ ;
- 2) a *posterior* inference of the scour depth  $D_{R1}$  based on the direct observation of scour at the same location 1 where the scour sensor is installed;
- 3) a *posterior* inference of the scour depth  $D_{R2}$  at the unmonitored location 2 based on the indirect observation of scour at the location 1 and water level at location 2.

The prior scour risk predictive model is based on the current scour risk assessment and management procedures used by transport agencies, where no information of scour depth enters the decision process and the monitored quantity that triggers bridge closures is the water level upstream of the bridge  $y_U$ . The posterior scour risk predictive model for a directly monitored location (i.e., denoted to as location 1) exploits information from the direct measurement of the relative scour depth ( $D_{R1}$ ) at the foundation of a bridge pier. Thus, the monitored quantity that triggers the bridge closure to traffic coincides with  $D_{R1}$  as there is no need to consider the water level as a proxy of scour. Finally, the posterior scour risk predictive model for an indirectly monitored location (i.e., denoted to as location 2) exploits information from the measurement of the scour depth at the location 1 and the water level observed upstream the location 2. The monitored quantity that triggers the bridge closure to traffic is the water level upstream of the bridge, as illustrated more in detail below.

The predictive model above is based on the BN-based framework developed in Maroni et al. [22]. The BN is a directed acyclic graph expressing the relationship between the various variables involved in the scour risk evaluation. The BN developed by Maroni et al. [22] is based on the BD 97/12 [11], which is the procedure followed by National Highways and Transport Scotland (TS) to assess the scour risk of their road bridges. In particular, starting from the river flow characteristics (such as river flow  $Q$ ), different models are applied to estimate the depth of flow upstream of the bridge  $y_U$ , and the two components of scour, constriction scour ( $D_C$ ) and local scour ( $D_L$ ), whose sum is equal to the total scour depth  $D_T$ . Fig. 3 shows an example of a BN used to estimate the scour depth at one bridge with two piers in the riverbed.

Manning equation is used to describe the relationship between  $Q$  and water depth  $y_U$  whereas a nonlinear system of three equations in three variables is developed to estimate the constriction scour depth  $D_C$  (i.e.,  $D_{C,ave}$  is the mean value of constriction scour depth). The system consists of the Colebrook–White equation, the conservation of fluid mass and the

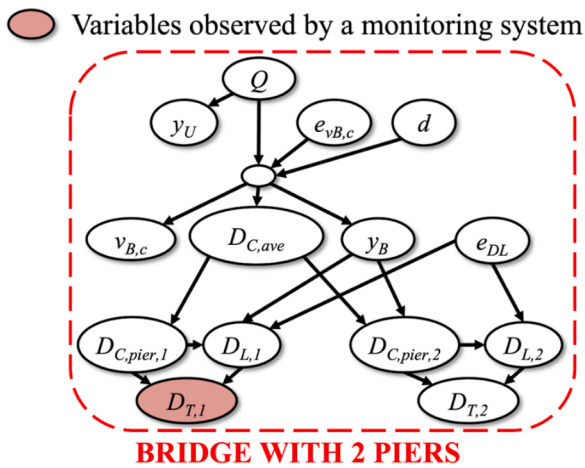


Fig. 3. BN for scour estimation at one bridge with two piers.

Bernoulli equation. The local scour depth  $D_L$  is calculated using an empirical formula based on the pier geometry, the pier alignment with respect to the water flow and the water depth itself. Model uncertainties are added to each model in the BN to describe the randomness of the estimation processes. Two types of error are defined: one expresses the systematic (perfectly correlated) error that affects the estimates when the model is used, and the other one represents a random (uncorrelated) error, that is, an additional error associated with the specific location (e.g., pier or bridge). This type of uncertainty is not displayed in the BN shown in Fig. 3 for the sake of clarity.

Many phenomena that affect the scour depth (e.g., unsteadiness of flow, variability of bed topography and riverbed soil conditions, etc.) are not explicitly modelled in the BN, but they are implicitly included via the abovementioned model uncertainties. The reader can refer to Maroni et al. [22] for more details about the definition of each model (including the parameters involved) and each uncertainty. These uncertainties are generally reduced by performing Bayesian Learning based on the available observations. The bias inherent to the scour models can also be corrected. It is noteworthy that the developed BN is a static one. A more rigorous approach for real-time scour risk assessment accounting for flow unsteadiness should be based on a dynamic BN (see e.g., [29–31]).

The BN can be used to perform a predictive analysis to estimate the a-priori probability density function (pdf) of the scour depth under an extreme flood given the pdf of the parent nodes of the network. It can also be employed for performing Bayesian learning, which in this context denotes the updating of the scour depth at any unmonitored location (i.e., location 2 in Fig. 3) in the bridge infrastructure network based on the measurement of scour at location 1. In fact, while at the monitored locations quite accurate scour estimates can be achieved, depending on the sensor accuracy, at the unmonitored ones it is still possible to observe a reduction of uncertainty thanks to the correlation existing between the scour depths at different locations.

### 3.2. Decision support system

The proposed DSS uses the outcomes of Bayesian learning for defining a monitoring-informed threshold (e.g., flood level marker  $\bar{y}_{SHM}$ ) for triggering the actions to be taken by the operator responsible for the bridge management. The rationale behind the DSS is that the knowledge of the actual scour depth at bridge foundations is characterised by significant uncertainty. Thus, the reduction of the uncertainty brought by sensor observations should also yield more accurate estimates of the critical scour levels (for location 1) or water levels (for location 2) triggering bridge closure, while maintaining the same target level of risk of bridge failure as the one inherent to current procedures.

At the base of the development of the DSS there is the choice of the implicit level of risk of bridge failure that the operator is willing to accept,  $P_{F0}$ . According to the simple decision tree depicted in Fig. 4, this risk threshold  $P_{F0}$  can be defined as the value of the probability of failure under the given flood event  $P_F$  that satisfies the following equation:

$$P_F C_F = C_{CB} \quad (1)$$

where  $C_{CB}$  denotes the losses due to the bridge closure, and  $C_F$  denotes the (direct and indirect) losses incurred by letting the traffic pass over the bridge when it fails. It is noteworthy that repair/reconstruction costs, which are present regardless of the action taken, are not shown in Fig. 4. The losses due to the reconstruction are indeed cancelled out due to the assumption of linear expected utility.

It is noteworthy that transport agencies and operators usually decide on bridge closure without carrying out an explicit risk/consequence analysis, but by comparing the water level  $y_U$  (i.e., water level upstream the bridge) with a level marker  $\bar{y}_{TA}$  based on experience and/or engineering judgement. However, introducing the probability of failure implicitly sought by transport agencies is essential for the development of the proposed DSS, which defines the adaptive water level threshold by targeting this probability of failure. The term “adaptive” is used because the DSS provides an updated water level threshold whose value may change with the information collected in real-time by scour sensors and the outcomes of Bayesian learning.

### 3.3. Failure probability

In general terms, the probability of failure due to scour at one pier of a bridge can be expressed as the probability that the scour demand is equal to or greater than the scour capacity, i.e., critical scour level resulting in bridge collapse. The relative values of the scour depth are considered hereinafter for expressing the scour demand and capacity, consistently with risk classifications. Both the demand and the capacity are random variables, due to the many uncertainties inherent to the problem. Thus, the probability of failure can be obtained as:

$$P_F = \int_{D_R} F_C(x) f_{D_R}(x) dx \quad (2)$$

where  $F_C(x)$  is the cumulative distribution function of the scour capacity, expressing the probability that the capacity is less than  $d_R$ , and  $f_{D_R}(x)$  is the probability density function of the relative scour demand.

For mathematical convenience, the relative scour capacity is assumed to follow a normal distribution with expected value  $E[D_{R,C}]$  and standard deviation  $\sigma_C$ . According to this model, the probability of failure  $P_F$  for a given relative scour depth can be expressed as:

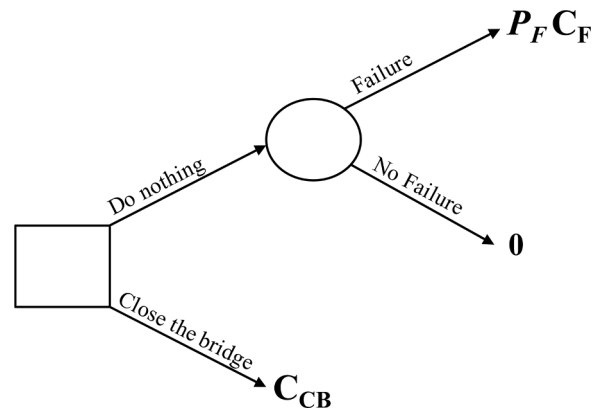


Fig. 4. Decision tree to define a threshold.



$$P_F(D_R) = P[C \leq D_R] = F_C(D_R) = \Phi\left(\frac{D_R - E[D_{R,C}]}{\sigma_C}\right), \quad (3)$$

where  $\Phi$  is the standard normal cumulative distribution function and  $E[D_{R,C}]$  is the mean scour capacity.

It is noteworthy that capacity models similar to the one employed here are widely used in other contexts such as Earthquake Engineering and are denoted to as fragility functions (see e.g., Gkimprixis et al., [32]. Fig. 5 shows the plot of Eq. (3) for two cases, corresponding to a mean value of scour capacity  $E[D_{R,C}] = 4.35$  and normal standard deviation  $\sigma_C = 0.66$  (i.e., fragility function 1) and to a mean value of scour capacity  $E[D_{R,C}] = 4.97$  and normal standard deviation  $\sigma_C = 1.15$  (i.e., fragility function 2). These values represent respectively a low and a large uncertainty in the bridge capacity. The value of  $E[D_{R,C}]$  and  $\sigma_C$  could be defined based on engineering judgement to yield acceptable values of the risk of failure for bridges belonging to different risk classes according to BD97/12. In the considered cases, the first fragility function is defined by assuming that the values of the probability of failure associated with the  $D_R$  levels separating class 2 from class 1 and class 3 from class 2 are respectively  $P_F = 10^{-1}$  and the  $P_F = 10^{-3}$ . The values assumed for fragility function 2 are  $P_F = 10^{-1}$  and  $P_F = 10^{-2}$ , respectively. The  $D_R$  levels defining the scour risk classes shown in Fig. 5 correspond to a bridge with a priority factor (Highway [11]) equal to 2.

Alternatively, the values of the parameters of the fragility curve for a specific bridge can be evaluated by performing numerical analyses under increasing levels of scour, such as in Tubaldi et al. [33] and Argyroudis et al. [34]. Nevertheless, the mean scour capacity  $E[D_{R,C}]$  is expected to be significantly higher than 1, even for the case of shallow foundations. This is because the scour models embedded in BD97/12 usually tend to overestimate significantly the scour demand for the critical flood level. Moreover, as illustrated in Tubaldi et al. [33], Scozzese et al. [35] and Tubaldi et al. [4], local scour holes usually have an inverted paraboloid shape, and a maximum scour depth significantly higher than the foundation depth is required to induce bridge collapse.

### 3.3.1. Prior failure probability

The relative scour demand consistent with the current decision system of transport agencies (relying on the fixed threshold  $\bar{y}_{TA}$ ) is defined

by the pdf of the relative scour depth corresponding to  $\bar{y}_{TA}$ . This distribution can be obtained via Bayesian learning by entering the observation  $\bar{y}_{TA}$  in correspondence of the node corresponding to the water level. This approach is consistent with the choice of TS of setting a red marker in correspondence of the water level  $\bar{y}_{TA}$  with a return period of 200 years. The obtained samples define the ‘‘a priori’’ distribution of the relative scour demand,  $D_{R,TA}$ , i.e., the relative scour pdf achieved from the BN without scour observations from scour sensors, that is, ‘‘a-priori’’ knowledge. The prior relative scour demand  $D_{R,TA}$  can be assumed to follow a normal distribution with an expected value  $E[D_{R,TA}]$  and standard deviation  $\sigma_{D_{R,TA}}$ .

Since both the prior demand and the capacity are normal random variables, the corresponding prior failure probability  $P_{F0}$  for a water level equal to  $\bar{y}_{TA}$  can be expressed:

$$P_{F0} = \Phi\left(\frac{E[D_{R,C}] - E[D_{R,TA}]}{\sqrt{\sigma_C^2 + \sigma_{D_{R,TA}}^2}}\right) \quad (4)$$

The next subsections discuss the calculation of the threshold for two cases a posteriori, corresponding respectively to a directly monitored location (i.e., location ‘‘1’’), and to an unmonitored location (i.e., location ‘‘2’’).

### 3.3.2. Posterior failure probability and threshold for a directly monitored location

Scour probes can achieve accurate scour measurements in the location where they are installed, and thus at these locations the scour demand is a deterministic variable  $D_{R1}$ , directly measured by the scour probe. The posterior failure probability associated with the updated scour depth distribution when the bridge location is directly monitored can be expressed as:

$$P_{F1} = \Phi\left(\frac{E[D_{R,C}] - D_{R1}}{\sigma_C}\right) \quad (5)$$

The failure probability must be the same as the one implicit in current procedures  $P_{F0}$  (i.e., the prior distribution); therefore, the critical mean level of scour  $\bar{D}_R$  that should trigger bridge closure can be found by solving the inverse reliability problem  $P_{F0} = P_{F1}$  for the unknown  $\bar{D}_R$ . This yields the following equation:

$$\frac{E[D_{R,C}] - E[D_{R,TA}]}{\sqrt{\sigma_C^2 + \sigma_{D_{R,TA}}^2}} = \frac{E[D_{R,C}] - D_{R1}}{\sigma_C} \quad (6)$$

The solution is:

$$D_{R1} = \bar{D}_R = E[D_{R,TA}]\gamma + E[D_{R,C}](1 - \gamma) \quad (7)$$

where the factor  $\gamma$  weights the total uncertainties in the posterior and prior distributions (e.g., relative scour demand and capacity):

$$\gamma = \frac{\sigma_C}{\sqrt{\sigma_C^2 + \sigma_{D_{R,TA}}^2}} \quad (8)$$

Since the monitoring system directly measures the scour at the monitored location there is no need to convert the critical mean level of scour  $\bar{D}_R$  into a critical water level in order to update a fixed flood level marker. Therefore, Eq. (7) provides a monitoring-based scour threshold that incorporates the uncertainty of the scour capacity and the piece of information provided by the scour observation (i.e., there is no uncertainty in the demand but in the capacity alone). It can be used under an extreme weather event to trigger bridge closure to traffic if the measured relative scour depth  $D_R$  exceeds  $\bar{D}_R$ . This updated scour threshold is valid only for monitored bridge locations, since for the unmonitored it is necessary to account also for the dispersion of the scour demand, as discussed in the following subsection.

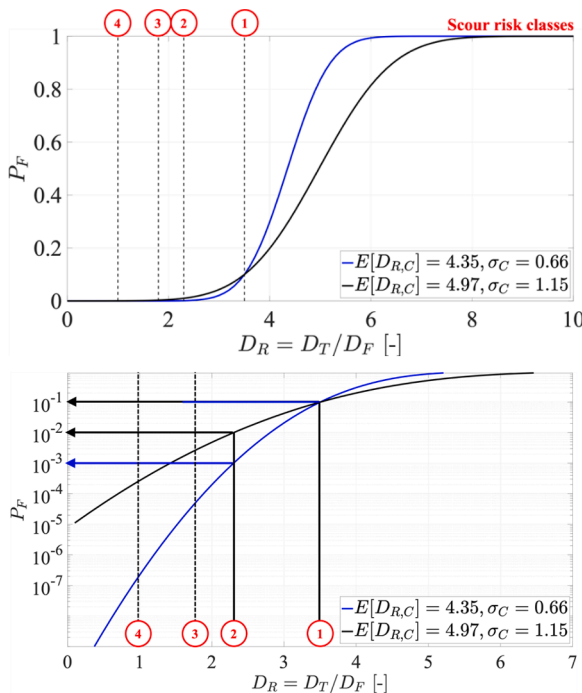


Fig. 5. Fragility functions for scour capacity C.

### 3.3.3. Posterior failure probability and threshold for an indirectly monitored location

In general, the scour depth is uncertain at locations not equipped with a scour monitoring system. This is also the case for indirect measurements of scour, e.g., using inclinometers or vibration-based identification techniques [17,20]. The posterior probabilistic distribution of the scour depth  $D_{R2|1}$ , which can be read as the posterior pdf of the scour at the location 2 (i.e., unmonitored) given the observation at location 1, can be assumed to follow a normal distribution with mean value  $E[D_{R2|1}]$  and normal standard deviation  $\sigma_{D_{R2|1}}$ .

The posterior failure probability associated with the updated scour depth distribution can be expressed as:

$$P_{F2|1} = \Phi \left( \frac{E[D_{R,C}] - E[D_{R2|1}]}{\sqrt{\sigma_C^2 + \sigma_{D_{R2|1}}^2}} \right) \quad (9)$$

where  $E[D_{R2|1}]$  is the expected value of the scour threshold that informs asset manager about the bridge closure to traffic.

Since the failure probability to be targeted by the new DSS should be the same as the one implicit in current procedures  $P_{F0}$  (i.e., the prior distribution), the critical mean level of scour  $\bar{D}_{R,SHM}$  that should trigger bridge closure can be found by solving the inverse reliability problem  $P_{F0} = P_{F2|1}$  for the unknown  $E[D_{R2|1}]$ . This yields the following equation:

$$\frac{E[D_{R,C}] - E[D_{R,TA}]}{\sqrt{\sigma_C^2 + \sigma_{D_{R,TA}}^2}} = \frac{E[D_{R,C}] - E[D_{R2|1}]}{\sqrt{\sigma_C^2 + \sigma_{D_{R2|1}}^2}} \quad (10)$$

The solution is:

$$E[D_{R2|1}] = \bar{D}_{R,SHM} = E[D_{R,TA}]\gamma + E[D_{R,C}](1 - \gamma) \quad (11)$$

where this time the factor  $\gamma$  is expressed as:

$$\gamma = \frac{\sqrt{\sigma_C^2 + \sigma_{D_{R2|1}}^2}}{\sqrt{\sigma_C^2 + \sigma_{D_{R,TA}}^2}} \quad (12)$$

Eq. (11) can also be rewritten as follows:

$$\frac{\bar{D}_{R,SHM}}{E[D_{R,TA}]} = \gamma + \frac{E[D_{R,C}]}{E[D_{R,TA}]}(1 - \gamma) \quad (13)$$

Since  $\gamma$  is expected to be less than 1, it can be concluded that for bridges that are classified at low risk of scour according to BD97/12 ( $E[D_{R,C}] \gg E[D_{R,TA}]$ ),  $\bar{D}_{R,SHM}$  is expected to be significantly higher than  $E[D_{R,TA}]$ , whereas for bridges at high risk of scour,  $\bar{D}_{R,SHM}$  can actually be lower than  $E[D_{R,TA}]$ .

In order to keep the same decision-making approach as the one currently adopted by agencies, the concept of monitoring-based flood level marker  $\bar{y}_{SHM}$  is introduced to update the fixed markers already defined for bridges at risk of scour. We label this variable as *adaptive threshold*. This marker is *adaptive* in the sense that can change continuously with the change of monitored value of  $D_{R1}$ . The adaptive threshold should be calculated from  $\bar{D}_{R,SHM}$  given by Eq. (11) by backward application of the predictive model. In order to invert the prediction model, it is convenient to replace it with a linear relationship whose parameters are identified by a simple linear regression analysis. For this purpose, Bayesian Learning is performed multiple times, considering several possible combinations of  $D_{R1}$  and  $y_{U2}$ , and evaluating the corresponding mean value and standard deviation of the posterior distribution of  $D_{R2|1}$ , respectively  $E[D_{R2|1}]$  and  $\sigma_{D_{R2|1}}$ . A multiple regression analysis is then performed to describe the variation of  $E[D_{R2|1}]$  with  $y_{U2}$  and  $D_{R1}$ :

$$E[D_{R2|1}] = f(y_{U2}, D_{R1}) = b_1 + b_2 D_{R1} + b_3 y_{U2} + b_4 D_{R1} y_{U2}. \quad (14)$$

A similar model can be used to fit  $\sigma_{D_{R2|1}}$ . However, as will be shown in the Case study section,  $\sigma_{D_{R2|1}}$  remains practically constant in all the investigated simulations.

By replacing  $E[D_{R2|1}]$  given by Eq. (14) in Eq. (11), a new expression of the water level  $y_{U2}$  can be defined, which satisfies the equality between the prior and posterior failure probabilities (i.e.,  $P_{F0} = P_{F2|1}$ ) and corresponds to the sought monitoring-based flood level marker:

$$y_{U2} = \bar{y}_{SHM} = \frac{E[D_{R,TA}]\gamma + E[D_{R,C}](1 - \gamma) - b_2 D_{R1} - b_1}{(b_3 + b_4 D_{R1})} \quad (15)$$

In summary, Eq. (15) provides an explicit expression of the adaptive threshold that should be used as a marker to decide whether to close the bridge or not, based on the indirect observation of scour depth  $D_{R1}$ . Eq. (15) assumes that the predictive model can be fit by a linear regression as in Eq. (14) and that the uncertainty of the prediction is effectively independent on the observation.

## 4. Case study

### 4.1. Description

The application of the monitoring-based DSS and the measurement-informed water level thresholds is illustrated considering the case study already presented in Maroni et al. [22]. This consists in a network of three scour-critical bridges managed by TS in south-west Scotland. The bridges cross the same river (River Nith) and only one pier of Bridge 1 (marked in green in Fig. 6b) is instrumented with a scour monitoring system [18]. The unmonitored location for each bridge (i.e., the piers located in the riverbed) is marked in blue in their descriptive figure. The main characteristics of these bridges are reported below:

- **Bridge 1:** A76 200 Nith bridge on River Nith in New Cumnock (Fig. 6). It is a 3-span (9.1 m, 10.7 m and 9.1 m) stone-masonry arch bridge, with two piers in the riverbed. Abutments and piers are all founded on spread footings on the natural riverbed.
- **Bridge 2:** A76 120 Guildhall bridge in Kirkconnel (Fig. 7). It is a 3-span (8.8 m, 11.3 m and 11.3 m) masonry arch bridge, with one pier in the riverbed. Both the abutments and the piers are founded on spread footings on natural ground.
- **Bridge 3:** A75 300 Dalscone bridge in Dumfries (Fig. 8). It is a 7-span (spans of 35 m and two of 28 m) steel-concrete composite bridge, with one pier in the riverbed. The abutments and piers are founded on pile foundations on natural ground.

The foundation depth  $D_F$  of the first two bridges is unknown because they were built in the 18th century. Therefore, in accord with BD97/12, a depth of 1 m is assumed in the calculation of the relative scour depth  $D_R$ . Instead, the Dalscone bridge is founded on sheet piling; according to procedure BD 97/12, in the case of a piled foundations  $D_F$  must be assumed equal to the underside depth of the pilecap, which for the Dalscone Bridge is 3 m.

### 4.2. Prior relative scour prediction

For each bridge, Transport Scotland has defined a fixed water level marker  $\bar{y}_{TA}$  as reported in Table 2. Based on these values, we wish to establish the mean value and standard deviation of the scour depth from the predictive model that are consistent with this water marker.

The probabilistic distribution of the scour demand consistent with the current decision system of transport agencies (relying on a fixed threshold  $\bar{y}_{TA}$ ) can be obtained via Bayesian learning by entering the observation  $\bar{y}_{TA}$  in correspondence of the node corresponding to the water level as shown in Fig. 9. The figure illustrates the application of

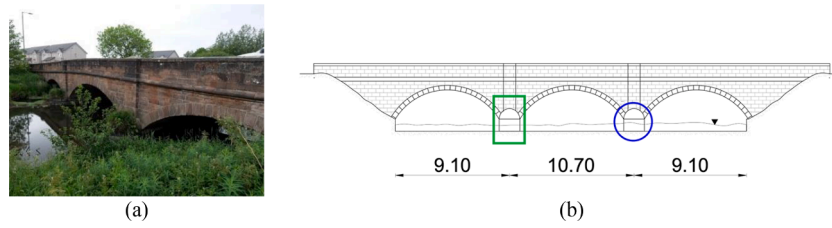


Fig. 6. (a) A76 200 Nith Bridge; and (b) bridge elevation.

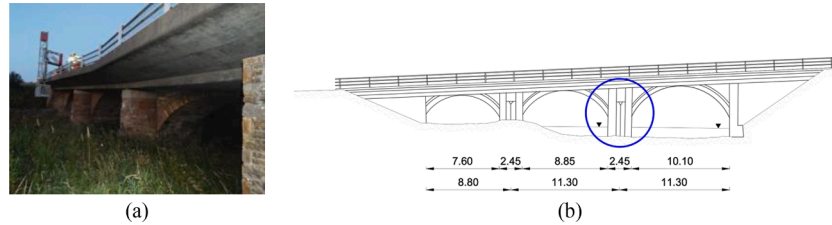


Fig. 7. (a) A76 120 Guildhall bridge; and (b) bridge elevation.

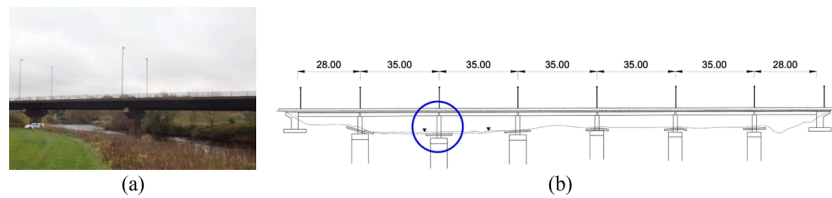


Fig. 8. (a) A75 300 Dalscone bridge; and (b) bridge elevation.

Table 2

Prior relative scour demand corresponding to  $\bar{y}_{TA}$ .

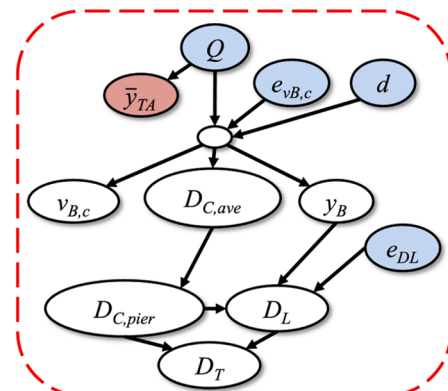
	Nith bridge	Guildhall bridge	Dalscone bridge
$\bar{y}_{TA}$	2.530	2.346	4.398
$E[D_{R,TA}]$	2.806	3.035	1.163
$\sigma_{D_{R,TA}}$	0.7389	0.8378	0.3274
<i>p-value</i>	0.1078	0.2034	0.1863

the BN-based probabilistic framework developed by Maroni et al. [22] for calculating the total scour depth experienced at the bridge pier when the water level is equal to fixed threshold  $\bar{y}_{TA}$ . The samples of the total scour depth, normalised by the foundation depth  $D_F$ , define the prior distribution of the relative scour demand,  $D_{R,TA}$ , i.e., the relative scour pdf achieved from the BN without scour observations from scour sensors. This corresponds to the “a-priori” knowledge of the scour depth.

Table 2 illustrates the parameters (i.e., expected value  $E[D_{R,TA}]$  and standard deviation  $\sigma_{D_{R,TA}}$ ) of the pdf of the prior relative scour demand corresponding to  $\bar{y}_{TA}$  for the three studied bridges. The Kolmogorov-Smirnov normality test [36] is performed on the samples of  $D_{R,TA}$  and the *p*-value returned by the test for the three cases are also reported in Table 2. These values are always higher than the value of 0.05, which is usually considered as level of significance, and thus the samples can be assumed to follow a normal distribution.

The results shown in Table 2, especially the ones in terms of standard deviation, confirm the significant uncertainty affecting the relationship between water levels and scour depths. Even when the water level is perfectly known, the scour depth exhibits a not-negligible dispersion, corresponding to a coefficient of variation in the range between 0.27 and 0.28. As expected, these values are lower than those obtained in Maroni et al. [22] by also considering the uncertainty in the water levels (of the order of 0.35–0.40).

- Root node
- Variables observed by a monitoring system



**NITH/GUILDHALL/DALSCONE BRIDGE**

Fig. 9. BNs for prior scour estimation at the bridge piers.  $Q$ : water flow;  $d$ : bed material grain size;  $v_{B,c}$ : scour threshold velocity;  $D_{C,ave}$ : average depth of constriction scour;  $y_B$ : depth of flow below the bridge;  $D_{C,pier}$ : depth of constriction scour at the pier;  $D_L$ : local scour depth;  $D_T$ : total scour depth;  $e_x$ : model uncertainties applied to the estimation models.

Fig. 10 illustrates the relationship between the samples of the relative total scour depth  $D_R$  and the upstream water level  $y_U$  for each of the three considered bridges. These samples have been obtained by performing predictive analysis, entering in the BN the discharge data recorded by gauging stations upstream of the bridges in the last 10 years.

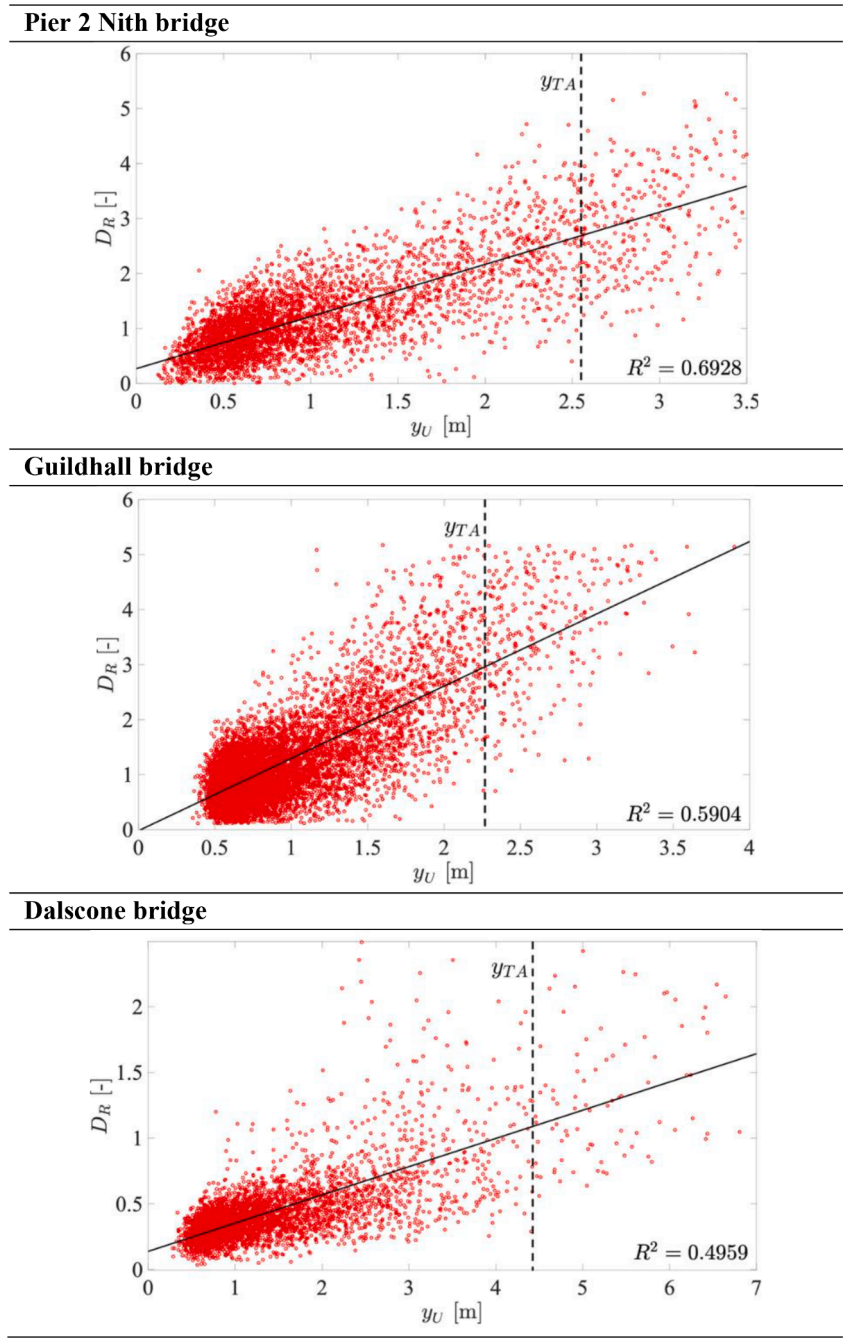


Fig. 10. Correlation between water level and total scour depth estimated by the BN-based framework.

It can be observed that different scour depths correspond to a given water level. Shown in Fig. 10 are also the fixed thresholds  $\bar{y}_{TA}$  obtained according to the TS procedure for each bridge. The corresponding values of the standard deviation of  $D_R$  are consistent with those presented in Table 2. These results confirm that the critical water level cannot be directly associated to a precise level of scour at the bridge foundations, because there is a weak correlation between water level and scour depth due to many uncertainties that affect the problem. In other words, water level is a very rough indicator of bridge scour risk.

4.3. Posterior inference at a directly monitored location

Table 3 shows the critical mean level of scour  $\bar{D}_R$  obtained with Eq. (7) that represents the scour threshold triggering the bridge closure to traffic when the bridge is monitored. The table provides two values of  $\bar{D}_R$

Table 3

Scour relative threshold triggering bridge closure when the scour depth at pier bridge is monitored.

		Nith bridge	Guildhall bridge	Dalscone bridge
Fragility function 1	$\gamma$	0.668	0.621	0.925
	$\bar{D}_R$	3.319	3.534	1.403
Fragility function 2	$\gamma$	0.841	0.808	0.973
	$\bar{D}_R$	3.150	3.407	1.266

because the scour threshold depends on  $\gamma$ , which in turn depends on  $\sigma_C$ , standard deviation of the two different fragility functions defining the relative scour capacity (e.g.,  $E[D_{RC}]=4.35$  and  $\sigma_C = 0.66$  for fragility function 1 and  $E[D_{RC}]=4.97$  and  $\sigma_C = 1.15$  for fragility function 2).



4.4. Posterior inference at an indirectly monitored location

For each of the three bridges considered, Bayesian Learning is performed multiple times to obtain posterior values of the expected value  $E[D_{R2|1}]$  and the standard deviation  $\sigma_{D_{R2|1}}$  of the scour depth  $D_{R2|1}$  at the unmonitored bridge locations, given different combinations of  $y_{U2}$  and  $D_{R1}$  (i.e., the scour depth measured at the base of pier 1 of the A76 200 Nith bridge). Fig. 11 shows the BNs deployed for the three Bayesian learning applications, corresponding to the updating of the total scour depth at the unmonitored locations. The application of the BN on the left corresponds to the scour estimation at pier 2 of the Nith bridge (i.e., location 2 is the unmonitored pier of the same bridge) whereas the application of the BN on the right corresponds to the estimation of the scour at underwater pier foundations of Guildhall and Dalscone bridges (i.e., location 2 is the pier of the unmonitored bridge). The three BN applications are all based on the total scour measured at pier 1 of Nith bridge and the water level at the corresponding bridges.

Table 4 shows the multiple linear fitting of the expected value  $E[D_{R2|1}]$  corresponding to Eq. (14) for the investigated bridges, including the four parameters that define the regression surface. The posterior standard deviation of the scour depth  $D_{R2|1}$  does not change significantly with  $y_{U2}$  and  $D_{R1}$  and it can be assumed constant for all the investigated cases.

4.5. Adaptive threshold

Fig. 12 illustrates the variation of the adaptive monitoring-based water level threshold  $\bar{y}_{SHM}$  for the three considered bridges, obtained by applying Eq. (15) assuming the fragility function with lower dispersion (i.e., fragility function 1 from Section 3.3). In the figures, the threshold  $\bar{y}_{SHM}$  is compared with the fixed threshold  $\bar{y}_{TA}$  implicitly chosen by TS.

The adaptive water level threshold decreases as the relative scour depth  $D_{R1}$  increases, i.e., values of  $\bar{y}_{SHM}$  higher than  $\bar{y}_{TA}$  are obtained for small values of  $D_{R1}$ , and values of  $\bar{y}_{SHM}$  lower than  $\bar{y}_{TA}$  are obtained for high values of  $D_{R1}$ . This is expected, since the scour depths at the unmonitored locations are correlated to the scour depth at the monitored one. Thus, when  $D_{R1}$  increases, also  $D_{R2|1}$  is expected to increase and thus the water level triggering bridge closure should decrease in order to ensure a consistent risk of failure for the bridge. It is worth noting that the adaptive threshold  $\bar{y}_{SHM}$  is always lower than the fixed threshold when the observed scour depth is equal to the critical mean level of scour  $\bar{D}_R$ . It is noteworthy that Dalscone bridge is founded on deep foundations (foundation depth  $D_F = 3$  m) whereas at Nith bridge  $D_F = 1$

m. Therefore, in order to avoid confusion between the representation scales of relative scour depth of location 2 ( $D_{R2}$  at Dalscone bridge) and 1 ( $D_{R1}$  at Nith bridge), the graph presented in Fig. 12c has a double x axis, the bottom one for the relative scour depth at location 1 (i.e., Nith bridge), and the top one for the relative scour depth at location 2 (i.e., Dalscone bridge). The first scale is used for the plot of  $\bar{y}_{SHM}$ , whereas the other scale is used for the plot of the other quantities.

Using the proposed adaptive threshold in the decision-making process is expected to reduce significantly the false positive cases (i.e., the unnecessary bridge closures) for low values of  $D_{R1}$  and the false negative cases for high values of  $D_{R1}$ . Table 5 compares the values of the adaptive and fixed threshold for the case of  $D_{R1} = 0$ . The relative increase of the threshold, when passing from a fixed to an adaptive one, is in the order of 70% for the A76 200 Nith bridge and around 40% for the other two bridges. The increase is highest for the case of Nith bridge because pier 1 is monitored, and the scour depth at pier 2 is highly correlated to the one at pier 1. Thus, higher uncertainty reductions are achieved in the estimates of the  $D_{R2|1}$  for this case compared to the other bridges.

Dalscone bridge presents a higher increase than Guildhall bridge since the former bridge is at very low risk of scour according to BD97/12 (i.e., ranked in risk class 5), whereas Guildhall is classified in risk class 3. In fact, according to Eq. (13), the scour threshold  $\bar{D}_{R,SHM}$  (and accordingly  $\bar{y}_{SHM}$ ) is expected to be significantly higher than  $E[D_{R,TA}]$  (and accordingly  $\bar{y}_{TA}$ ) in bridges that are classified at low risk of scour (i.e., for a high  $E[D_{R,C}] / E[D_{R,TA}]$  ratio).

Fig. 13 compares the values of the adaptive thresholds of Fig. 12 normalised with respect to the corresponding values of  $\bar{y}_{TA}$  given in Table 2. The sensitivity of the normalised adaptive threshold to the value of  $D_{R1}$  (measured by the slope of the curves plotted in Fig. 13) is higher for Nith bridge than for the other two bridges. This is expected considering that the monitoring system is installed at Nith bridge. Furthermore, the graph below shows that the Nith bridge also experiences the higher increase in the threshold for lower values of  $D_{R1}$ . This could be again explained by the more confident estimation of scour at pier 2 (i.e., pier 1 is directly monitored) than the ones performed at the other two unmonitored bridges. The higher confidence in the knowledge of the scour depth yields higher values of water level threshold by keeping the same level of risk implicitly chosen by transport agencies. On the contrary, but the same reason, in the case of high levels of observed scour  $D_{R1}$ , the normalised water level threshold at Nith bridge is lower than the ones at the other two bridges.

In order to appreciate the sensitivity of the adaptive threshold to the specific fragility function, Fig. 14 plots the adaptive threshold for two different fragility functions defining the relative scour capacity (e.g.,  $E$

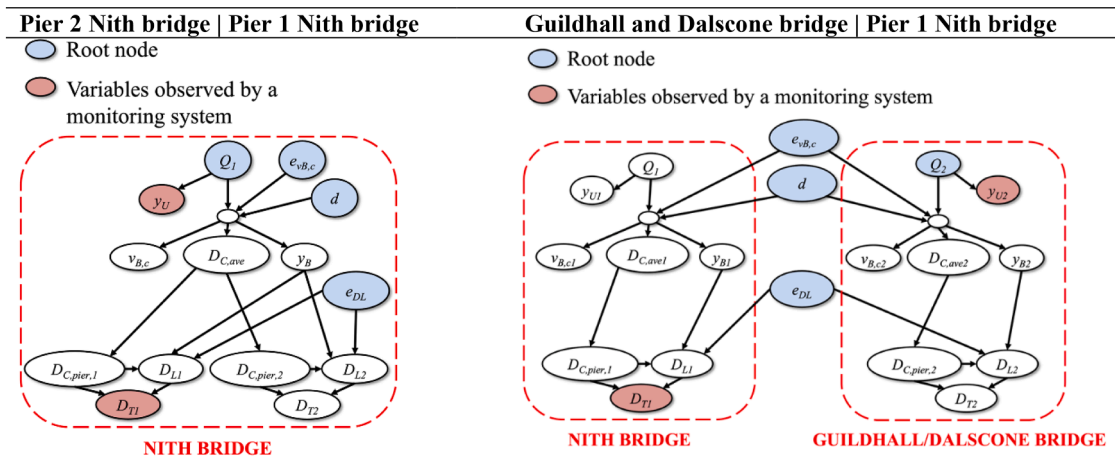
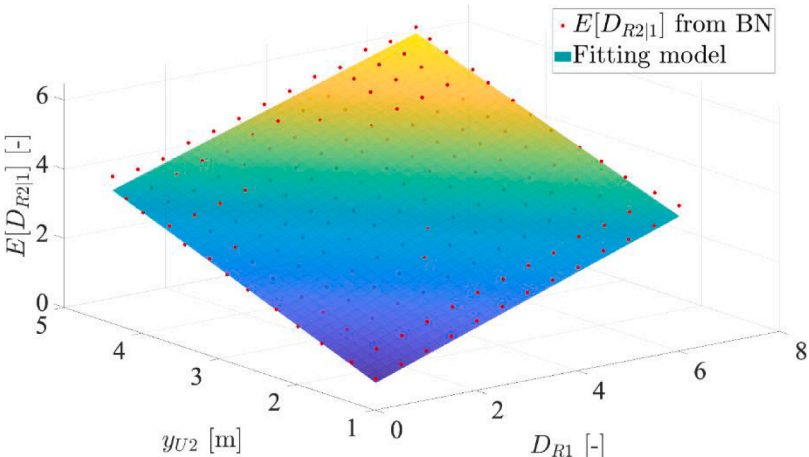
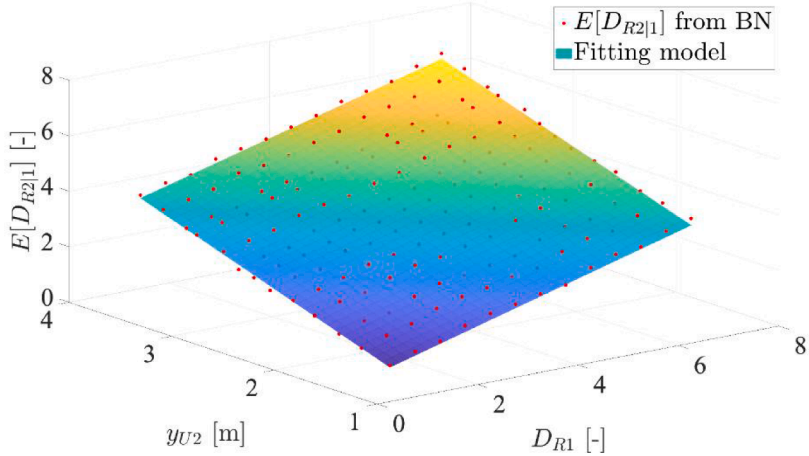
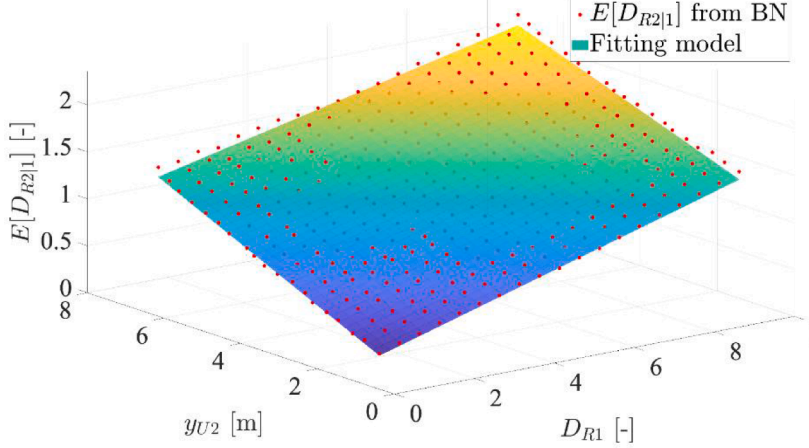


Fig. 11. The three BN applications for posterior scour estimation at the bridge piers starting from scour measured at pier 1 of Nith bridge and the water level at the corresponding bridges.

**Table 4**  
Multiple linear fitting of the expected value of relative scour depth  $D_{R2|1}$  (Eq.(14)) for the three studied bridges.

Pier 2 Nith bridge   Pier 1 Nith bridge & water level Nith bridge	$b_1 = -0.7579$ $b_2 = 0.5676$ $b_3 = 0.9091 \text{ m}^{-1}$ $b_4 = -0.0361 \text{ m}^{-1}$ $\sigma_{D_{R2 1}} = 0.1563$
	
Guildhall bridge   Pier 1 Nith bridge & water level Guildhall bridge	$b_1 = -0.8751$ $b_2 = 0.5114$ $b_3 = 1.2569 \text{ m}^{-1}$ $b_4 = -0.0792 \text{ m}^{-1}$ $\sigma_{D_{R2 1}} = 0.2791$
	
Dalscone bridge   Pier 1 Nith bridge & water level Dalscone bridge	$b_1 = 0.0032$ $b_2 = 0.1302$ $b_3 = 0.1974 \text{ m}^{-1}$ $b_4 = -0.0050 \text{ m}^{-1}$ $\sigma_{D_{R2 1}} = 0.0822$
	

$[D_{R,C}] = 4.35$  and  $\sigma_C = 0.66$  for Fragility function 1 and  $E[D_{R,C}] = 4.97$  and  $\sigma_C = 1.15$  for Fragility function 2). It can be noted that the two curves almost overlap meaning that the knowledge level of the capacity of the bridge against scour has a minor effect on the water level threshold  $\bar{y}_{SHM}$ . In fact, the adaptive thresholds obtained with the two different capacity models are not significantly different from each other.

### 5. Conclusions

This paper presents a rationale to establish an adaptive water level threshold  $\bar{y}_{SHM}$  triggering bridge closure due to scour risk, which accounts for indirect information from scour monitoring sensors. A BN-based approach is used for predicting and updating the probabilistic distribution of scour at unmonitored bridge locations based on the available observations (e.g., scour depth at the monitored location). The updated, adaptive measurement-informed water level threshold  $\bar{y}_{SHM}$  is

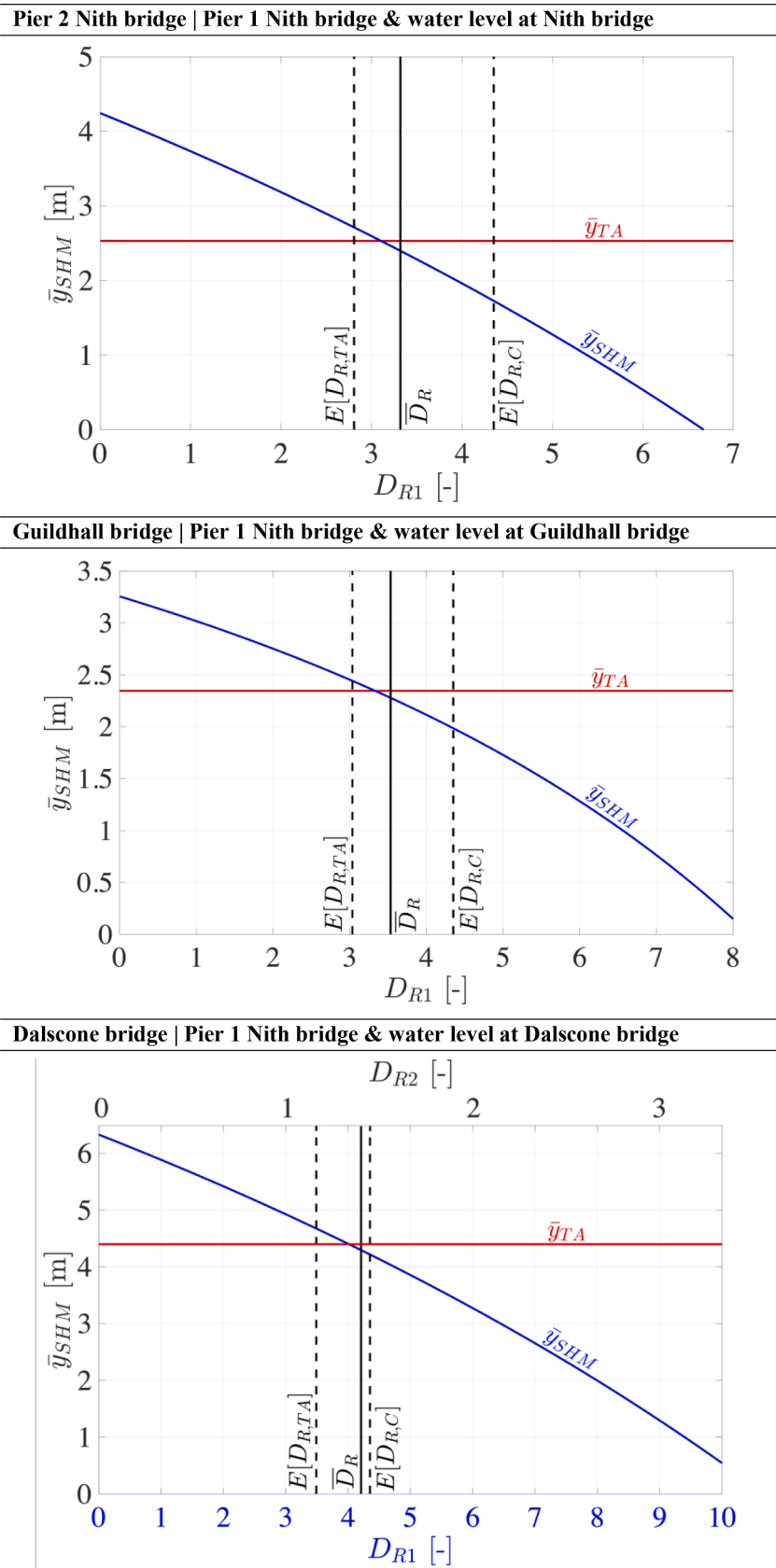
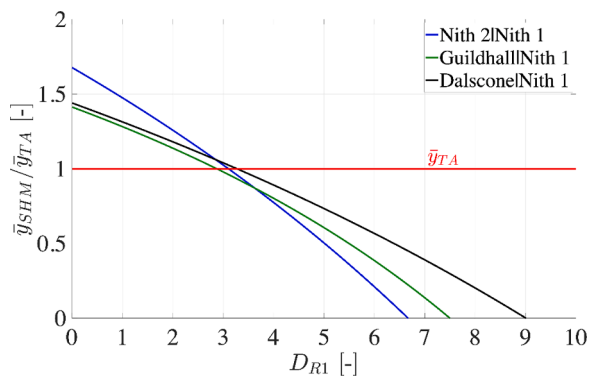


Fig. 12. Adaptive monitoring-based water level threshold from BN's outcomes of unmonitored components.

**Table 5**

Fixed water level threshold  $\bar{y}_{TA}$  vs adaptive monitoring-based water level threshold  $\bar{y}_{SHM}$  when  $D_{R1} = 0$ .

	Nith bridge – Pier 2	Guildhall bridge	Dalscone bridge
<b>Fixed water level threshold – <math>\bar{y}_{TA}</math> [m]</b>	2.530	2.346	4.398
<b>Adaptive monitoring-based water level threshold – <math>\bar{y}_{SHM}</math> (<math>D_{R1} = 0</math>) [m]</b>			
$\bar{y}_{SHM}$	4.24	3.26	6.33
<b>Relative increase</b>	+68%	+39%	+44%



**Fig. 13.** Comparison of the monitoring-based water level thresholds  $\bar{y}_{SHM}$  normalised with respect to the correspondence  $\bar{y}_{TA}$ .

estimated by targeting the same probability of bridge failure as that implicit in current bridge flood management plans, based on flow depth expected under a 1 in 200yrs flood event. We illustrate the application of the proposed DSS on a small network consisting of three bridges at risk of scour managed by Transport Scotland in south-west Scotland.

Based on the study results, the following conclusions can be drawn:

- i. The adaptive water level threshold  $\bar{y}_{SHM}$  decreases for increasing levels of the relative scour depth  $D_{R1}$  at the monitored pier. Compared to the fixed markers  $\bar{y}_{TA}$  currently considered by Transport Scotland, higher values of the water level triggering bridge closure are obtained for small values of  $D_{R1}$ , and lower values for high values of  $D_{R1}$ .
- ii. The adaptive threshold  $\bar{y}_{SHM}$  depends on the ratio between the median scour capacity and the median scour demand, that in turn, depend on the bridge prior risk of failure. In particular, for bridges with low risk of failure due to scour, the adaptive threshold departs significantly from the fixed threshold while this difference is less significant for bridges at high scour risk of failure.
- iii. The difference between the adaptive threshold  $\bar{y}_{SHM}$  and the fixed marker  $\bar{y}_{TA}$  is more significant if the indirect observation is made on a pier of the same bridge.
- iv. The choice of fragility function used for describing the scour capacity does not significantly affect the adaptive threshold  $\bar{y}_{SHM}$ . Therefore, we can safely establish a reasonable value of adaptive threshold regardless our knowledge of the scour bridge capacity.

The general method and formulation introduced in this paper are suitable for extension to any decision problems that include observations from different types of sensors and multiple decision options, comprising long-term and/or emergency risk management of bridges. These additional topics will be investigated in future studies.

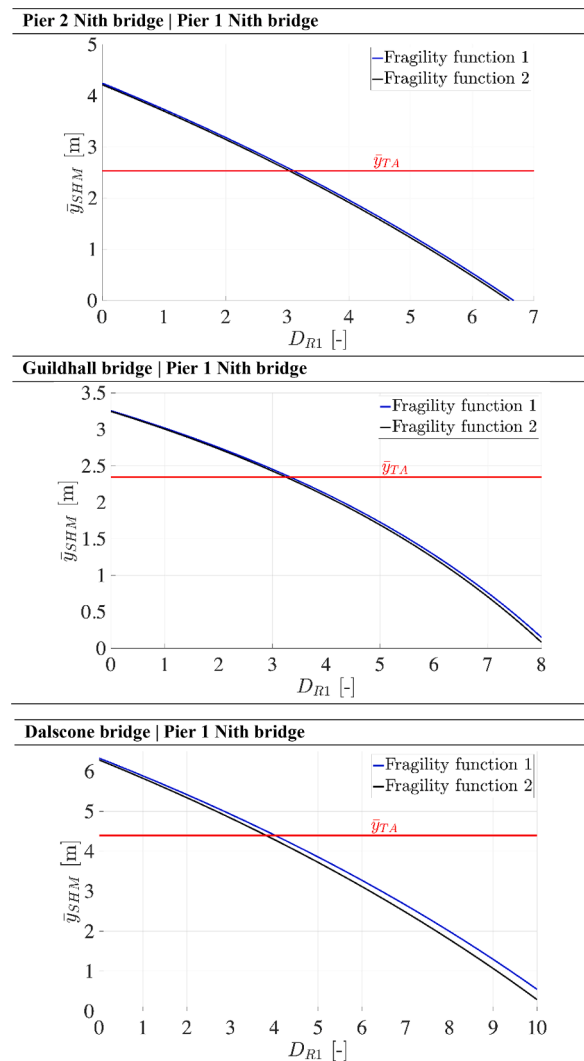


**Fig. 14.** Adaptive monitoring-based water level threshold from BN's outcomes of unmonitored components.

**Disclosure statement**

No potential conflict of interest was reported by the authors.

**Funding**

This study was supported by the NERC ERIIP (Environmental Risk to Infrastructure Innovation Programme) [grant no. NE/R009090/1]; the National Centre for Resilience (NCR) [grant no. NCR2021-003]; and the Scottish Road Research Board (SRRB) [Decision Support System based on “adaptive” Flood Level Markers].

**CRedit authorship contribution statement**

**Andrea Maroni:** Conceptualization, Methodology, Data curation, Software, Writing – original draft, Writing – review & editing. **Enrico Tubaldi:** Conceptualization, Methodology, Writing – original draft, Writing – review & editing, Supervision. **Hazel McDonald:** Resources, Conceptualization, Methodology. **Daniele Zonta:** Conceptualization, Methodology, Writing – review & editing, Supervision.



## Declaration of Competing Interest

The authors declare that they have no known competing financial interests or personal relationships that could have appeared to influence the work reported in this paper.

## Data availability

Data will be made available on request.

## References

- [1] Kirby A, Roca M, Kitchen A, Escarameia M, Chesterton O. Manual on scour at bridges and other hydraulic structures. Ciria C742; 2015.
- [2] Pizarro A, Manfreda S, Tubaldi E. The science behind scour at bridge foundations: a review. *Water* 2020;12(2):374.
- [3] Richardson EV, Davis SR. Evaluating scour at bridges (HEC-18). US Department of Transportation. Federal highway administration. 4th edn. Colorado: FHWA NHI; 2001. p. 01. -001.
- [4] Tubaldi E, White CJ, Patelli E, et al. Invited perspectives: challenges and future directions in improving bridge flood resilience. *Nat Hazards Earth Syst Sci* 2022;22(3):795–812.
- [5] Van Leeuwen Z, Lamb R. Flood and scour related failure incidents at railway assets between 1846 and 2013. Railway safety & standards board. 2014.
- [6] Briaud JL, Brandimarte L, Wang J, D'odorico P. Probability of scour depth exceedance owing to hydrologic uncertainty. *Georisk* 2007;1(2):77–88.
- [7] Wardhana K, Hadipriono FC. Analysis of recent bridge failures in the United States. *J Perform Constr Facil* 2003;17(3):144–50.
- [8] Dikanski H, Hagen-Zanker A, Imam B, Avery K. Climate change impacts on railway structures: bridge scour. Proceedings of the Institution of Civil Engineers-Engineering Sustainability 2016;170(5):237–48. Thomas Telford Ltd.
- [9] Dikanski H, Imam B, Hagen-Zanker A. Effects of uncertain asset stock data on the assessment of climate change risks: a case study of bridge scour in the UK. *Struct Saf* 2018;71:1–12.
- [10] Kay AL, Crooks SM, Davies HN, Reynard NS. project R10023PUR, CEH Wallingford. An assessment of the vulnerability of Scotland's river catchments and coasts to the impacts of climate change: Work Package 1 Report to Scottish Environment Protection Agency; 2011. p. 219. August 2011.
- [11] Agency Highway. The assessment of scour at and other hydraulic actions at highway structures - procedure BD97/12. vol. 3 of design manual for roads and bridges. London, UK: The Stationery Office Ltd; 2012.
- [12] Johnson PA, Clopper PE, Zevenbergen LW, Lagasse PF. Quantifying uncertainty and reliability in bridge scour estimations. *J Hydraul Eng* 2015;141(7):04015013.
- [13] Pizarro A, Tubaldi E. Quantification of modelling uncertainties in bridge scour risk assessment under multiple flood events. *Geosciences* 2019;9:445. -15.
- [14] Tubaldi E, Macorini L, Izzuddin BA, Manes C, Laio F. A framework for probabilistic assessment of clear-water scour around bridge piers. *Struct Saf* 2017;69:11–22.
- [15] Giordano PF, Prendergast LJ, Limongelli MP. A framework for assessing the value of information for health monitoring of scoured bridges. *J Civil Struct Health Monitor* 2020;10(3):485–96.
- [16] Argyroudis SA, Mitoulis SA, Winter MG, Kaynia AM. Fragility of transport assets exposed to multiple hazards: state-of-the-art review toward infrastructural resilience. *Reliab Eng Syst Saf* 2019;191:106567.
- [17] Prendergast LJ, Gavin K. A review of bridge scour monitoring techniques. *J Rock Mech Geotech Eng* 2014;6(2):138–49.
- [18] Maroni A, Tubaldi E, Ferguson NS, Tarantino A, McDonald H, Zonta D. Electromagnetic sensors for underwater scour monitoring. *Water Sens* 2020;20(15):4096.
- [19] Achillopoulou DV, Mitoulis SA, Argyroudis SA, Wang Y. Monitoring of transport infrastructure exposed to multiple hazards: a roadmap for building resilience. *Sci Total Environ* 2020;746:141001.
- [20] Tubaldi E., Maroni A., Ferguson N.S., Zonta D. Report on critical review of alternative techniques for bridge scour monitoring. Project report. National Centre for Resilience; 2020. <https://eprints.gla.ac.uk/225801/1/225801.pdf>. Last access: 26/06/2023.
- [21] Martínez-Martínez LH, Delgado-Hernández DJ, de-León-Escobedo D, Flores-Gomora J, Arteaga-Arcos JC. Woody debris trapping phenomena evaluation in bridge piers: a Bayesian perspective. *Reliab Eng Syst Saf* 2017;161:38–52.
- [22] Maroni A, Tubaldi E, Val DV, McDonald H, Zonta D. Using Bayesian Networks for the assessment of underwater scour for road and railway bridges. *Struct Health Monitor* 2020. <https://doi.org/10.1177/1475921720956579>.
- [23] Transport Scotland. Scour management strategy and flood emergency plan. Glasgow, UK: Trans Scotland; 2018.
- [24] Hamill L. Bridge hydraulics. London, UK: E & FN Spon; 1999.
- [25] Melville BW, Coleman SE. Bridge scour. Water Resources Publication; 2000.
- [26] Briaud JL, Gardoni P, Yao C. Statistical, risk, and reliability analyses of bridge scour. *J Geotech Geoenviron Eng* 2014;140(2):04013011.
- [27] Bolduc LC, Gardoni P, Briaud JL. Probability of exceedance estimates for scour depth around bridge piers. *J Geotech Geoenviron Eng* 2008;134(2):175–84.
- [28] RAIB. Structural failure caused by scour at lamington viaduct, south Lanarkshire 31 December 2015, (Report 22/2016). Rail accident investigation branch. Department for Transport; 2016.
- [29] Ching J, Chen YC. Transitional Markov chain Monte Carlo method for Bayesian model updating, model class selection, and model averaging. *J Eng Mech* 2007;133(7):816–32.
- [30] Cai B, Zhang Y, Wang H, Liu Y, Ji R, Gao C, Kong X, Liu J. Resilience evaluation methodology of engineering systems with dynamic-Bayesian-network-based degradation and maintenance. *Reliab Eng Syst Saf* 2021;209:107464.
- [31] Kammouh O, Gardoni P, Cimellaro GP. Probabilistic framework to evaluate the resilience of engineering systems using Bayesian and dynamic Bayesian networks. *Reliab Eng Syst Saf* 2020;198:106813.
- [32] Gkimpraxis A, Tubaldi E, Douglas J. Comparison of methods to develop risk-targeted seismic design maps. *Bull Earthq Eng* 2019;17:3727–52.
- [33] Tubaldi E, Macorini L, Izzuddin BA. Three-dimensional mesoscale modelling of multi-span masonry arch bridges subjected to scour. *Eng Struct* 2018;165:486–500.
- [34] Argyroudis SA, Mitoulis SA. Vulnerability of bridges to individual and multiple hazards-floods and earthquakes. *Reliab Eng Syst Saf* 2021;210:107564.
- [35] Scozzese F, Ragni L, Tubaldi E, Gara F. Modal properties variation and collapse assessment of masonry arch bridges under scour action. *Eng Struct* 2019;199:109665.
- [36] Massey J F. The Kolmogorov-Smirnov test for goodness of fit. *J Am Statist Assoc* 1951;46(253):68–78.